Peer-reviewed version available at *Atmosphere* **2018**, *9*, 144; doi:10.3390/atmos9040144

Hazard Quotients, Hazard Indexes, and Cancer Risks of Toxic Metals in PM_{10} during Firework Displays

Siwatt Pongpiachan[1,3*], Akihiro Iijima[2], and Junji Cao[3]

[1]NIDA Center for Research & Development of Disaster Prevention & Management, School of Social and Environmental Development, National Institute of Development Administration (NIDA), 118 Moo 3, Sereethai Road, Klong-Chan, Bangkapi, Bangkok, 10240, THAILAND

[2]Department of Regional Activation, Faculty of Regional Policy, Takasaki City University of Economics, 1300 Kaminamie, Takasaki, Gunma 370-0801, JAPAN

[3]SKLLQG, Institute of Earth Environment, Chinese Academy of Sciences (IEECAS), Xi'an, 710075, CHINA

* Corresponding Author: Tel: 00 66 2 727 3113; Fax: 00 66 2 732 0276; Email: pongpiajun@gmail.com

ABSTRACT

Bonfire night is a worldwide phenomenon given to numerous annual celebrations characterised by bonfires and fireworks. Since Thailand has no national ambient air quality standards for metal particulates, it is important to investigate the impacts of particulate injections on elevations of air pollutants and ecological health impacts resulting from firework displays. In this investigation, Pb and Ba were considered potential firework tracers because their concentrations were significantly higher during the episode and lower than/comparable with minimum detection limits during other periods, indicating that their elevated concentrations were principally due to pyrotechnic displays. Pb/Ca, Pb/Al, Pb/Mg, and Pb/Cu can be used to pin-point emissions from firework displays. Air mass backward trajectories (72 h) from the Hybrid Single-Particle Lagrangian Integrated Trajectory (HYSPLIT) model indicated that areas east and north-east of the study site were the main sources for the air transportation. Although the combined risk associated with levels of Pb, Cr, Co, Ni, Zn, As, Cd, V, and Mn was far below the standards mentioned in international guidelines, the lifetime cancer risks associated with As and Cr levels exceeded US-EPA guidelines, and may expose inhabitants of surrounding areas of Bangkok to elevated cancer risk.

Keywords: Firework displays, Toxic metals, Principal component analysis, Risk assessment, Hazard quotient, Hazard index

Highlights

- Pyrotechnics emit PM_{10}-bound heavy metals that degrade ambient air quality
- Pb/Ca, Pb/Al, Pb/Mg, and Pb/Cu ratios can pinpoint emissions from firework displays
- Pb and Ba are possible tracers, with elevated concentrations during firework displays
- PM_{10} metals in ambient air are mainly crustal emissions regardless of firework events
- Limited combined risk associated with Pb, Cr, Co, Ni, Zn, As, Cd, V, and Mn levels
- As and Cr levels exceed US-EPA guidelines for lifetime cancer risk

INTRODUCTION

Over the last few decades there has been increasing interest in the adverse public health impacts of exposure to ambient toxic chemicals, principally in relation to carcinogenicity and mutagenicity (Pongpiachan, 2013a,b; Pongpiachan et al., 2013, 2015a,b, 2017a,b,c,d). Another central concern of ambient air quality studies is the chemical compositions of particulate metals. It is important to note that most toxic metals are preferentially present in finer aerosols, since they have lower densities and greater surface area per unit of volume and organic matter content (Charlesworth et al., 2003; Madrid et al., 2008; Yatkin and Bayram, 2008a,b). Recent studies underline the adverse health effects of exposure to particulate metals (Fang et al., 2013; Kong et al., 2011; Lu et al., 2014; Wu et al., 2015). To the best of our knowledge, there are very few publications on PM_{10}-bound heavy metals in Southeast Asian countries, which have a combined population of 651 million. Consequently, it seems profitable to monitor the levels of such metals in ambient air. Such data would be essential for public administrative bodies, such as the Environmental Protection Agency (EPA) or Pollution Control Department (PCD), for preparing amendments or revisions to air quality standards, as well as establishing baseline data for atmospheric research communities.

Previous studies have highlighted traffic emissions (Christoforidis and Stamatis, 2009; Duong and Lee, 2011; Johansson et al., 2009; Ndiokwere, 1984), solid waste incinerators (Jianguo et al., 2004; Zhang et al., 2008), thermal power plants (Meij and te Winkel, 2007; Reddy et al., 2005; Sushil and Batra, 2006), industrial boilers (Dahl et al., 2009; Yoo et al., 2002), open burning of e-waste and municipal solid waste (Fujimori et al., 2016; Wang et al., 2017), and forest fires (Betha et al., 2013; Breulmann et al., 2002) as major sources of heavy metals in ambient air. Despite the large number of published studies on the emission sources of selected metals in particulate matter, their behaviours in tropical regions remain unclear, especially in Southeast Asian countries, where few databases of particulate metals have been published and made publicly accessible.

During the past few years, several studies have examined the enhanced levels of toxic pollutants in ambient air during firework displays (Camilleri and Vella, 2010; Pongpiachan et al., 2017a; Seidel and Birnbaum, 2015). The literature also highlights the impacts of firework displays as one of the main contributors of specific metal particulates in ambient air (Feng et al., 2016; Tsai et al., 2012; Wang et al., 2007). Despite several investigations highlighting the importance of traffic emissions as a source of chemical pollutants in Bangkok (Pongpiachan, 2013b; Pongpiachan et al., 2013, 2015a, 2017b), there is no research on the effects of the "Loy Krathong Festival" (LKF) on the increase of selected metals in ambient air. It is a tradition for Thai people to float Krathongs (i.e., floating baskets) on a river, to pay respect to the spirit of the Thai river goddess or Phra Mae Kongkha. People generally launch elaborate fireworks on the evening of the full moon in the 12th month of the traditional Thai lunar calendar. In Northern Thailand, LKF is locally acknowledged as "Yi Peng", which is one of the most memorable Lanna festivals throughout the year, combined with Khomloi (i.e., Lanna-style sky lanterns) and firework displays. Hence, it is evident that more field research is required to elucidate the influences of firework displays on selected metal profiles. The main goals of this study are to: (*i*) compare selected metal profiles before and after firework displays; (*ii*) investigate the influences of firework displays on the behaviours of selected PM_{10}-bound metals; and (*iii*) calculate hazard quotients, hazard indexes, and cancer risks associated with toxic metals in PM_{10} before and after the bonfire night episodes in the centre of Bangkok Metropolitan.

2. MATERIALS & METHODS

2.1. Air quality observation sites

This study examined the impacts of fireworks displays on ambient air quality in Bangkok according to the mass concentrations of PM_{10} and their chemical characteristics, including selected metals. Data on ambient air quality were collected from four Pollution Control Department (PCD) Air

Quality Observatory Sites, namely MBK (MBKOS), Ramkamhaeng (RKOS), Land Development Department (LDDOS) and Victory Monument Observatory Site (VMOS), which were carefully chosen for the assessment of selected metals in PM_{10}. The positions of the four air quality monitoring sites in relation to a public firework display platform are illustrated in Fig. 1. Intensive monitoring campaigns were performed consecutively, before and after the bonfire night event during LKF, Father's Day (5th of December), and New Year's Eve celebrations from 2012 to 2013, forming a database of 62 individual PM_{10} samples (50 collected before, and 12 after the firework display).

High-volume air samplers (TE-6001; Graseby-Anderson) were used to obtain unmanned 24 h samples for PM_{10} at the four sampling sites, yielding volumes of approximately 1,632 m^3 for each 24 h sample. PM_{10} were collected on 20×25 cm Whatman glass fibre filters (GFFs) at a flow rate of approximately 1.133 m^3 min^{-1} (i.e., 40 cfm): Sample air flow rate was calibrated for standard temperature and pressure conditions. A more comprehensive explanation of the air sampling method was given in "Compendium Method IO - 2.2. Sampling of Ambient Air for PM_{10} using an Andersen Dichotomous Sampler" (Winberry et al., 1988).

2.2. Chemical analysis of selected metals

Chemical preparations, coupled with analytical instrument optimisation, were comprehensively described in earlier reports (Iijima et al., 2009, 2010). In summary, PM_{10} filters were positioned in PTFE vessels and digested in a mixture of 2 mL hydrofluoric acid (50% atomic absorption spectrometry grade; Kanto Chemical Co., Inc.), 3 mL nitric acid (60% electronic laboratory grade; Kanto Chemical Co., Inc.), and 1 mL hydrogen peroxide (30% atomic absorption spectrometry grade; Kanto Chemical Co., Inc.) in a microwave digestion system (Multiwave; Anton Parr, GmbH). The microwave oven was operated at 700 W for 10 min, and 1000 W for a further 10 min. Hydrofluoric acid was evaporated by heating the sample solutions at 200 °C on a hot plate. The digested solutions were further diluted with 0.1 mol L^{-1} nitric acid (prepared from 60% nitric acid)

was the added to obtain a 50 mL sample. The concentrations of 31 selected metals (Li, Be, Na, Mg, Al, K, Ca, Sc, V, Cr, Mn, Fe, Co, Ni, Cu, Zn, As, Se, Rb, Sr, Y, Zr, Mo, Cd, Sn, Sb, Cs, Ba, Tl, Pb, and Bi) were determined by inductively coupled plasma mass spectrometry (Agilent 7500cx; Agilent Technologies, Inc.). All the chemical analytical processes were verified using Standard Reference Material (SRM) 1648 (i.e., urban particulate matter) provided by the US National Institute of Standards and Technology (NIST). The analytical results showed good agreement with the certified or reference values. The instrumental detection limits of the 31 selected metals are displayed in Table S1 (see Supplementary Material).

2.3. Health risk assessment of selected metals

Concentration and time are frequently used to depict exposure, where amount/mass characterises dose, and the time parameter allows calculation of the dose rate. In order to evaluate the health threats associated with PM_{10}, the average exposure to selected metals by inhalation (D_{inh}) for both children and adults, based on individual's body weight during a given period, is computed using Eq. (1) (Feng et al., 2016; Granero and Domingo, 2012; Kong et al., 2012;):

$$D_{inh} = \frac{C \times InhR \times EF \times ED}{BW \times AT}$$

Equation (1)

Where D_{inh} is exposure by respiratory inhalation (mg kg^{-1} day^{-1}); *InhR* is inhalation rate (7.6 and 20 m^3 day^{-1} for children ($InhR_{child}$) and adults ($InhR_{adult}$), respectively); EF is exposure frequency (day $year^{-1}$); ED is exposure duration (6 years for children (ED_{child}), 24 years for adults (ED_{adult}), respectively); BW is average body weight (15 kg for children (BW_{child}), 70 kg for adults (BW_{adult})); AT is the averaging time (for non-cancer toxic risks, AT (days)=ED×365; for cancer risks, AT (days)=70×365); C is exposure-point concentration, which is calculated by the upper limit of the 95% confidence interval for the mean (mg m^{-3}). In this study, the lifetime average daily dose

Preprints (www.preprints.org) | NOT PEER-REVIEWED | Posted: 20 March 2018 doi:10.20944/preprints201803.0171.v1

Peer-reviewed version available at Atmosphere 2018, 9, 144; doi:10.3390/atmos9040144

(*LADD*) of selected metals through inhalation is employed for evaluating health risk, as described in Eq. (2).

$$LADD = \frac{C \times EF}{AT} = \left(\frac{InhR_{child} \times ED_{child}}{BW_{child}} + \frac{InhR_{adult} + ED_{adult}}{BW_{adult}}\right)$$

Equation (2)

It is also important to introduce the concept of a hazard quotient. Theoretically, a hazard quotient (*HQ*) is the ratio of the potential exposure to a selected metal, relative to the level at which no adverse effects are expected. After D_{inh} is computed, *HQ* can be obtained using Eqs. (3) and (4):

$$HQ = \frac{D_{inh}}{RfD}$$

Equation (3)

$$HI = \sum HQ_i$$

Equation (4)

RfD is the reference dose (mg kg^{-1} day^{-1}). Hazard Index (*HI*) is calculated by summing the individual *HQ*s to assess the total health risks of all selected target metals. *RfD* values from Feng et al. (2016) were used for Pb (3.52×10^{-3}), Cr (2.86×10^{-5}), Co (5.71×10^{-6}), Ni (2.06×10^{-2}), Zn (3.01×10^{-1}), As (3.01×10^{-4}), Cd (1×10^{-3}), V (7×10^{-3}), and Mn (1.4×10^{-5}). If the calculated *HQ* is <1, then no adverse health effects are expected because of exposure. Conversely, if *HQ* is >1, then negative health impacts are possible.

Cancer risk (R_t) is computed using Eqs. (5) and (6):

$$R = LADD \times SF_a$$

Equation (5)

$$R_t = \sum R$$

Preprints (www.preprints.org) | NOT PEER-REVIEWED | Posted: 20 March 2018 doi:10.20944/preprints201803.0171.v1

Peer-reviewed version available at Atmosphere 2018, 9, 144; doi:10.3390/atmos9040144

Equation (6)

Where SF_a is a slope factor (mg kg^{-1} day^{-1}). The SF_a values used for Cr, Co, Ni, As, and Cd are 42, 9.8, 0.84, 15.1, and 6.4, respectively (Feng et al., 2016).

2.4. Enrichment factors of selected metals

During the past few decades, enrichment factor (*EF*) has been comprehensively adopted to evaluate the influences of vehicular exhausts, industrial releases, and mining coupled with ore processing, on atmospheric metals (Li et al., 2012; Wang et al., 2014; Zhang et al., 2015). Despite some uncertainties regarding the selection criteria for the reference elements, Al, Fe, and Si are regularly employed for *EF* computations (López et al., 2005). In this investigation, Fe was selected as a reference element, presuming the subtle influences of contaminated Fe and the upper continental crustal composition provided by Rudnick (2003). The *EF* of an element *E* in a PM_{10} sample can be explained as

$$EF = \frac{(E/R)_{Air}}{(E/R)_{Crust}}$$

Equation (7)

Where *R* is a reference element. In the case of *EF* values close to one, the crust can be considered as the main contributor. Additionally, SPSS (version 13) was adopted for Pearson correlation analysis (SLRA) and *t*-tests.

2.5. Estimation of mineral matter in PM_{10}

The evaluation of mineral matter (*MIN*) in PM_{10} was conducted using the common oxides of Ti, Al, Mn, Mg, Ca, Na, K, and Fe, which were summed (represented as MIN) and then subsequently computed using Eq. (8) (Feng et al., 2016; Kong et al., 2015; Terzi et al., 2010).

$$MIN = 1.89 \times Al + 1.59 \times Mn + 1.67 \times Mg + 1.95 \times Ca + 1.35 \times Na + 1.21 \times K + 1.43 \times Fe$$

Equation (8)

Preprints (www.preprints.org) | NOT PEER-REVIEWED | Posted: 20 March 2018 doi:10.20944/preprints201803.0171.v1

Peer-reviewed version available at Atmosphere 2018, 9, 144; doi:10.3390/atmos9040144

It is important to note that trace elements (*TE*) is the sum of all other metals except the above elements in MIN, as shown in Eq. (9).

$$TE = Li + Be + Sc + V + Cr + Co + Ni + Cu + Zn + As + Se + Rb + Sr + Y + Zr + Mo + Cd + Sn + Sb + Cs + Ba + Tl + Pb + Bi - MIN$$

Equation (9)

For Ca, a factor of 1.95 is adopted herein because of the presence of CaO and $CaCO_3$.

2.6. Back trajectory analysis

Backward trajectories, starting from each receptor site, were calculated using the HYSPLIT_4 (Hybrid Single-Particle Lagrangian Integrated Trajectory) Model with GDAS (Global Data Analysis System) one-degree gridded meteorological dataset (Draxler and Hess, 1998). The 72-hour backward trajectories with 6 h temporal resolutions were computed at starting time of 02:00 UTC (local time in Thailand is UTC + 7 hours) on each sampling day. Since back trajectories are sensitive to differences in starting height (Draxler, 2003), the trajectories were tested starting from multiple heights of 1000 m, 1500 m, and 2000 m above sea level to confirm the uncertainty due to the inadequate spatial and/or temporal resolution of the input data.

3. RESULTS AND DISCUSSION

Table 1 shows the statistical descriptions of selected PM_{10}-bound metals, as well as the *t*-test analysis during the FDP and NDP, as mentioned previously in section 2.1. The arithmetic means of the 31 selected metal particulate contents ranged from 0.061±0.0086 ng m^{-3} (Be) to 2,096±548 ng m^{-3} (Ca) for FDP, and from 0.062±0.017 ng m^{-3} to 2,794±929 ng m^{-3} (Ca) for NDP (see Table 1). Of the 31 selected metals, although seven (Al, Ca, Sc, Cr, Y, Ba, and Pb) showed significant variations (p <0.05) in mean concentrations between FDP and NDP (see Table 1), only two of those (Ba and Pb) represented significant increases. These findings were in good agreement with previous studies highlighting that Ba and Pb can be considered as firework tracers (Kumar et al., 2016; Tsai et al., 2012; Vecchi et al., 2008). The fact that some earlier studies highlight Sr (Kumar et al., 2016;

Peer-reviewed version available at Atmosphere 2018, 9, 144; doi:10.3390/atmos9040144

Vecchi et al., 2008), Mg and K (Kumar et al., 2016; Tsai et al., 2012), and K, Ba, Sr, Cd, S, and P (Kumar et al., 2016) as firework tracers may simply reflect the complexity of metal salts generally employed to generate colours in firework displays, which include $SrCO_3$ (red), $CaCl_2$ (orange), $NaNO_3$ (yellow), $BaCl_2$ (green), copper $CuCl_2$ (blue), and a mixture of metal salts including Sr and Cu (purple colour).

It is well known that selected metals can be categorised into two clusters: crustal metals (including Al, Ca, Fe, Mg, K, and Na), which could be principally attributed to high loading of crustal dust; and anthropogenic metals (such as Zn, As, Pb, V, Ti, Cr, Mn, Ni, Sr, Cu, Li, Cd, and Co), which originate from human activities (e.g., traffic exhaust, industrial emissions, burning of fossil fuels) (Pan et al., 2015). In this study, the atmospheric concentrations of crustal metals (i.e., the sum of Al, Ca, Fe, Mg, K, and Na) were 6,582 ng m^{-3} for FDP and 7,438 ng m^{-3} for NDP. Interestingly, the particulate contents of anthropogenic metals (i.e., the sum of Zn, As, Pb, V, Ti, Cr, Mn, Ni, Sr, Cu, Li, Cd, and Co) were 510 ng m^{-3} for FDP and 468 ng m^{-3} for NDP. Since the anthropogenic metals were slightly higher in FDP, it seems rational to interpret particle injections triggered by firework displays as a main contributor to atmospheric concentrations of anthropogenic metals during the LKF period. These findings are also in good agreement with the finding that the *TE* concentration (see Eq. (9)) detected in FDP (i.e., 581 ng m^{-3}) was slightly higher than in NDP (i.e., 526 ng m^{-3}).

As illustrated in Fig. 2, two near-identical patterns (represented as percentage contributions) of particulate selected metals were detected during the FDP and NDP episodes, both of which followed the sequence: Ca>Na>K>Fe>Al>Mg>Zn>Cu>Pb. The similar decreasing sequence of selected metals between the two episodes highlights the relatively homogeneous distribution of the 31 target compounds throughout the ambient air of Bangkok during the observation periods. Since previous studies report that vehicle exhaust is the main emission source of air pollutants in Bangkok (Pongpiachan, 2013b; Pongpiachan and Iijima, 2016; Pongpiachan et al., 2013, 2015a,

2017a), it appears rational to interpret the identical distribution patterns of the selected metal compositions between the two episodes as resulting from the effects of road traffic emissions rapidly overwhelming other potential contributors during the sampling period. Further evaluations of particulate metal injections triggered by firework displays were conducted by applying the concept of diagnostic binary ratios, which will be described in section 3.1.

3.1. Diagnostic binary ratios of selected metals

Although the application of diagnostic binary ratios is frequently criticised as a reliable tool for identifying the emission sources of air pollutants (Galarneau et al., 2008), this technique has still been widely used in numerous studies tracing particulate metals in ambient air during the past few years (Font et al., 2015; Hieu and Lee, 2010; Weckwerth, 2001). A simple binary ratio of two or three selected metals is sensitive to physicochemical transformations, and emission source strengths that can occur in the ambient air commonly involve metal contributions from numerous sources; consequently, a comprehensive consideration of several metal ratios can provide a broader picture for potential source identification. In this study, Ba and Pb were the only two metals that showed significantly higher concentrations during the firework display episodes. It is also worth mentioning that Ca, Na, K, Fe, Al, Mg, Zn, and Cu were the eight most abundant metals observed in both episodes. For these reasons, 16 pairs of selected metals were selected as potential tracers for firework emissions (see Table 2). The 16 metal ratios fell within the ranges 0.033□0.56 and 0.017□0.35 for FDP and NDP, respectively. As illustrated in Fig. 3, emissions of Li–Cs showed strong correlation (R=0.92, n=50, p<0.0001) followed by Li–Tl (R=0.92, n=50, p<0.0001), Al–Y (R=0.93, n=50, p<0.0001), V–Ni (R=0.91, n=50, p<0.0001), Mn–Cs (R=0.97, n=50, p<0.0001), Mn–Tl (R=0.90, n=50, p<0.0001), and Cu–Mo (R=0.92, n=50, p<0.0001). Consequently, Li/Cs, Li/Tl, Al/Y, V/Ni, Mn/Cs, and Mn/Tl were tested to evaluate their potential as firework tracers. Unfortunately, the FDP/NDP ratios of these six metal ratios were ≈1 and therefore inappropriate as firework tracers. Interestingly, only four metal ratios observed in FDP (i.e., Pb/Ca, Pb/Al, Pb/Mg,

and Pb/Cu) were approximately two times higher than in NDP. Additionally, eight metal ratios (Ba/Ca, Ba/Na, Ba/K, Ba/Fe, Ba/Al, Ba/Mg, Ba/Zn, and Ba/Cu) had ratios <1.6. Since Se and Cd were the two metals with the largest enrichment factors (Fig. 4), a binary ratio of Se/Cd was also computed in both sampling campaigns. Regrettably, the FDP/NDP ratio of Se/Cd was close to one (i.e., 0.8), indicating its unsuitability for characterising firework displays.

3.2. Enrichment factors of selected metals

As shown in Fig. 4, the logarithmic *EF*s of the 31 selected metals in PM_{10} detected at both monitoring campaigns from November 2012 to December 2013 followed the sequence: Se>Sb>Cd>Bi>Cu>Sn>Pb>Mo>Zn>As>Tl>Ba>Ni>V>Rb>Ca>Cs>K>Na>Zr>Mn>Li>Be>Sr>Co >Cr>Fe>Y>Sc>Mg>Al. These findings can be categorised into four groups as an arbitrary scale, based on earlier reports (Karageorgis et al., 2009; Pongpiachan and Iijima, 2016). Firstly, Se, Sb, and Cd were excessively enriched (i.e., 3<Log(*EF*)<4). Secondly, Bi, Cu, Sn, Pb, Mo, and Zn were highly enriched (i.e., 2<Log(*EF*)<3). Thirdly, As and Tl were substantially enriched (i.e., 1<Log(*EF*)<2). Fourthly, Ba, Ni, V, Rb, Ca, Cs, K, Na, Zr, Mn, Li, Be, Sr, Co, Cr, Fe, Y, Sc, Mg, and Al were not enriched (i.e., Log(*EF*)<1). It is important to note that almost 35% of Log(*EF*) were <1; only 10% were >3; and 55% were <1. It is well known that numerous phenomena, such as vehicular exhaust, construction dust, crustal sources, industrial emissions, burning of agricultural waste, re-suspension of road dust, and sea salt aerosols, can greatly alter the Log(*EF*) values.

Since the Log(*EF*) values of five metals (Co, Cr, Y, Sc, and Mg) approached zero (i.e., *EF* values close to one) in both sampling periods, the crust is concluded to be the major source. Although previous studies highlighted Mg as a firework tracer (Kumar et al., 2016; Tsai et al., 2012), the present findings suggest that Mg might not be a good indicator of firework displays. The extremely high Log(*EF*) values of Se, Sb, and Cd are explained in terms of vehicular emissions, and are in reasonably good accordance with previous studies (Lough et al., 2005; Almeida et al., 2006;

Crawford et al., 2007; Pongpiachan and Iijima, 2016). Additionally, the extremely low Log(*EF*) values observed for Al (i.e., FDP: -0.59; NDP: -0.54) observed here are consistent with earlier studies (Pongpiachan and Iijima, 2016; Wu et al., 1994). Terrestrial soil releases of particulate Al are the most reasonable interpretation of these exceedingly low Log(*EF*) values detected in both sampling episodes.

The back trajectory analysis reveals prevailing easterly and north-easterly surface winds during the observation period (see Figs. S1–S5). It is obvious that the majority of the prevailing winds passed over potential anthropogenic emission sources (i.e., the Special Economic Zones (SEZ) in Cambodia) before reaching the study site. Although total employment in all of Cambodia's SEZs is currently approximately 68,000, this represents just under 1% of total employment and 3.7% of total secondary industry employment in Cambodia (Warr and Menon, 2016). Transport statistics (http://apps.dlt.go.th/statistics_web/brochure/cumcar12.pdf) show 7,523,381 vehicles registered in Bangkok as of 31 December 2012. The total number of vehicles in Bangkok is almost double that for the whole of Cambodia, which was calculated as 338,791 (i.e., population× number of vehicles per capita: (16,132,910×21)/1,000) (http://www.nationmaster.com/country-info/stats/Transport/Road/Motor-vehicles-per-1000-people).
Hence, it appears reasonable to assume that the easterly winds were comparatively less influenced by anthropogenic emissions. These findings were consistent with the relatively low Log(*EF*) values observed in the present study, highlighting that crustal emissions dominated the ambient air quality of Bangkok during the observation period.

3.3. Hazard quotients, hazard indexes, and cancer risks of selected metals

Statistics for $D_{inh\text{-}children}$, $D_{inh\text{-}adults}$, $HQ_{children}$, HQ_{adult}, and *LADD* are shown in Table 3, including during both monitoring campaigns. As clearly displayed in Table 3, the risk levels of Pb, Cr, Co, Ni, Zn, As, Cd, V, and Mn through the inhalation exposure system in both FDP and NDP were in

Preprints (www.preprints.org) | NOT PEER-REVIEWED | Posted: 20 March 2018 doi:10.20944/preprints201803.0171.v1

Peer-reviewed version available at Atmosphere 2018, 9, 144; doi:10.3390/atmos9040144

357 the range of 3.52×10^{-7}~6.75×10^{-3} and 1.99×10^{-7}~3.80×10^{-3} for children and adults, respectively.
358 Both values were much lower than the acceptance risk of 1. It should be noted that the sequence of
359 risk levels for the non-carcinogenic heavy metals was Mn>Cr>Co>As>Pb>Cd>V>Zn>Ni, which
360 differ from those for $PM_{2.5}$ in Xinxiang (Zn>Pb>As>V>Cr>Mn>Ni>Cd>Co) reported by Feng et al.
361 (2016). This discrepancy might be explained by some differences in particle size distributions
362 (Marcazzan et al., 2001; Samara and Voutsa, 2005; Wang et al., 2013) and emission source
363 characteristics between Bangkok and Xinxiang. It is worth mentioning that the sum of the risk
364 levels (*HI*) for the nine heavy metals were 7.28×10^{-3} and 4.10×10^{-3} for children and adults,
365 respectively. These are clearly less than 0.1 and much less than 1; moreover, they are 33 and 32
366 times lower than the risk levels reported for Xinxiang for children and adults, respectively. Since
367 the HQ_{children} values were almost double the HQ_{adult} values for both monitoring periods, it appears
368 reasonable to mention that children are more vulnerable than adults to the noncancerous effects of
369 these nine non-carcinogenic heavy metals (Yang et al., 2014). This can be attributed to their
370 mouthing behaviours, whereby children's hand-to-mouth activities represent a major pathway of
371 chemical exposure (Pongpiachan, 2016; Pongpiachan et al., 2017a).
372
373 The *LADD* of Pb, Cr, Co, Ni, Zn, As, Cd, V, and Mn, and the cancer risk (R_t) (see Eq. 6) associated
374 with As, Cd, Cr, Ni, and Co exposure via respiration, are also displayed in Table 3. The sequence of
375 *R* values (see Eq. 5) during the FDP was As>Cr>Cd>Co>Ni, which differs from those observed in
376 Xinxiang (i.e., As>Cd>Cr>Ni>Co) by Feng et al. (2016). It is important to note that the
377 carcinogenic risks associated with As, Cd, Cr, Ni, and Co were all $>10^{-6}$; in particular, As and Cr
378 were 180 and 145 times greater than internationally accepted precautionary or threshold values for
379 cancer risk (Feng et al., 2012; Wang et al., 2007). Additionally, the carcinogenic risks for Ni (FDP:
380 5.94×10^{-6}; NDP: 4.51×10^{-6}) and Co (FDP: 6.51×10^{-6}; NDP: 6.55×10^{-6}) were slightly higher than the
381 accepted value of 10^{-6}. Overall, the lifetime cancer risks of particulate As, Cd, Cr, Ni, and Co
382 noticeably surpass the US-EPA guidelines, and it seems rational to conclude that these may expose

neighbouring residents in Bangkok to enhanced risk of cancer.

4. CONCLUSIONS

The atmospheric concentrations, hazard quotients, hazard indexes, and cancer risks of 31 selected metals present in PM_{10} were investigated during firework display and non-display periods in Bangkok. Only Ba and Pb were significantly higher during the firework display periods. These results were consistent with earlier findings indicating that these two metals can be acknowledged as firework tracers. Since the Pb/Ca, Pb/Al, Pb/Mg, and Pb/Cu ratios were approximately two times higher during the firework display period, it appears reasonable to apply these four diagnostic binary ratios as potential firework tracers, particularly in the case of Bangkok. Enrichment factors highlighted the importance of crustal emissions as a main contributor of particulate metals in ambient air of Bangkok regardless of firework events. No significant differences in risk levels were observed for Pb, Cr, Co, Ni, Zn, As, Cd, V, or Mn during firework episodes. Although *HI* values observed in both sampling campaigns were much lower than international guidelines, the carcinogenic risks associated with As, Cd, Cr, Ni, and Co all exceeded the acceptable level of 10^{-6}, raising public health concerns over increased cancer risk among surrounding residents in Bangkok.

5. ACKNOWLEDGEMENT

The authors acknowledge support for this study from the Information Technology Foundation under the Initiative of Her Royal Highness Princess Maha Chakri Sirindhorn; the National Science and Technology Development Agency (NSTDA); the Chinese Academy of Sciences (IEECAS); and the National Institute of Development Administration (NIDA). The authors acknowledge all research staff at the Pollution Control Department (PCD), The Ministry of Natural Resources and Environment of the Kingdom of Thailand for their assistance with field sampling of PM_{10}.

REFERENCES

Almeida, S.M., Pio, C.A., Freitas, M.C., Reis, M.A., Trancoso, M.A., 2006. Source apportionment of atmospheric urban aerosol based on weekdays/weekend variability: evaluation of road re-suspended dust contribution. Atmos. Environ., 40, 2058-2067.

Betha, R., Pradani, M., Lestari, P., Joshi, U. M., Reid, J. S., Balasubramanian, R., 2013. Chemical speciation of trace metals emitted from Indonesian peat fires for health risk assessment. Atmospheric Res. 122, 571-578.

Breulmann, G., Markert, B., Weckert, V., Herpin, U., Yoneda, R., Ogino, K., 2002. Heavy metals in emergent trees and pioneers from tropical forest with special reference to forest fires and local pollution sources in Sarawak, Malaysia. Sci Total Environ. 285(1), 107-115.

Camilleri, R., Vella, A.J., 2010. Effect of fireworks on ambient air quality in Malta. Atmos. Environ. 44(35), 4521-4527.

Charlesworth, S., Everett, M., McCarthy, R., Ordóñez, A., de Miguel, E., 2003. A comparative study of heavy metal concentration and distribution in deposited street dusts in a large and a small urban area: Birmingham and Coventry, West Midlands, UK. Environ. Int. 29; 563–573.

Christoforidis, A., Stamatis, N., 2009. Heavy metal contamination in street dust and roadside soil along the major national road in Kavala's region, Greece. Geoderma, 151(3), 257-263.

Crawford, J., Chambers, S., Cohen, D.D., Dyer, L., Wang, T., Zahorowski, R., 2007. Receptor modelling using positive matrix factorization, back trajectories and Radon-222. Atmos. Environ. 41, 6823-6837.

Dahl, O., Nurmesniemi, H., Pöykiö, R., Watkins, G., 2009. Comparison of the characteristics of bottom ash and fly ash from a medium-size (32 MW) municipal district heating plant incinerating forest residues and peat in a fluidized-bed boiler. Fuel Process. Technol. 90(7), 871-878.

Draxler, R.R., Hess, G.D., 1998. An overview of the HYSPLIT_4 modelling system for trajectories, dispersion and deposition. Aust. Meteorol. Mag. 47, 295-308.

Draxler, R.R., 2003. Evaluation of an ensemble dispersion calculation. J. Appl. Meteor. 42, 308-317.

Duong, T. T., Lee, B. K., 2011. Determining contamination level of heavy metals in road dust from busy traffic areas with different characteristics. J. Environ. Manage. 92(3), 554-562.

Fang, W., Yang, Y., Xu, Z., 2013. PM_{10} and $PM_{2.5}$ and health risk assessment for heavy metals in a typical factory for cathode ray tube television recycling. Environ. Sci. Technol. 47(21), 12469-12476.

Feng, J.L., Sun, P., Hu, X.L., Zhao, W., Wu, M.H., Fu, J.M., 2012. The chemical composition and sources of $PM_{2.5}$ during the 2009 Chinese New Year's holiday in Shanghai. Atmos. Res. 118, 435-444.

Feng, J., Yu, H., Su, X., Liu, S., Li, Y., Pan, Y., Sun, J. H., 2016. Chemical composition and source apportionment of PM 2.5 during Chinese spring festival at Xinxiang, a heavily polluted city in north China: Fireworks and health risks. Atmospheric Res. 182, 176-188.

Font, A., de Hoogh, K., Leal-Sanchez, M., Ashworth, D.C., Brown, R.J., Hansell, A.L., Fuller, G.W., 2015. Using metal ratios to detect emissions from municipal waste incinerators in ambient air pollution data. Atmos. Environ. 113, 177-186.

Fujimori, T., Itai, T., Goto, A., Asante, K.A., Otsuka, M., Takahashi, S., Tanabe, S., 2016. Interplay of metals and bromine with dioxin-related compounds concentrated in e-waste open burning soil from Agbogbloshie in Accra, Ghana. Environ. Pollut. 209, 155-163.

Galarneau, E., 2008. Source specificity and atmospheric processing of airborne PAHs: implications for source apportionment. Atmos. Environ. 42(35), 8139-8149.

Granero, S., Domingo, J., 2012. Levels of metals in soils of Alcala de Henares, Spain: human health risks. Environ. Int. 28, 159-164.

Hieu, N.T., Lee, B.K., 2010. Characteristics of particulate matter and metals in the ambient air from a residential area in the largest industrial city in Korea. Atmospheric Res. 98(2), 526-537.

Iijima, A., Sato, K., Fujitani, Y., Fujimori, E., Saitoh, Y., Tanabe, K., Ohara, T., Kozawa, K., Furuta, N., 2009. Clarification of the predominant emission sources of antimony in airborne particulate matter and estimation of their effects on the atmosphere in Japan. Environ. Chem. 6, 122-135.

Iijima, A., Sato, K., Ikeda, T., Sato, H., Kozawa, K., Furuta, N., 2010. Concentration distributions of dissolved Sb(III) and Sb(V) species in size-classified inhalable airborne particulate matter. J. Anal. At. Spectrom. 25, 356-363.

Jianguo, J., Jun, W., Xin, X., Wei, W., Zhou, D., Yan, Z., 2004. Heavy metal stabilization in municipal solid waste incineration flyash using heavy metal chelating agents. J. Hazard. Mater. 113(1), 141-146.

Johansson, C., Norman, M., Burman, L., 2009. Road traffic emission factors for heavy metals. Atmos. Environ. 43(31), 4681-4688.

Karageorgis, A.P., Katsanevakis, S., Kaberi, H., 2009. Use of enrichment factors for the assessment of heavy metal contamination in the sediments of Koumoundourou Lake, Greece. Water Air Soil Pollut. 204, 243-258.

Kong, S., Lu, B., Ji, Y., Zhao, X., Chen, L., Li, Z., Han, B., Bai, Z., 2011. Levels, risk assessment and sources of PM 10 fraction heavy metals in four types dust from a coal-based city. Microchem. J. 98(2), 280-290.

Kong, S.F., Lu, B., Ji, Y.Q., Zhao, X.Y., Bai, Z.P., Xu, Y.H., Liu, Y., Jiang, H., 2012. Risk assessment of heavy metals in road and soil dust within $PM_{2.5}$, PM_{10} and PM_{100} fractions in Dongying city, Shandong Province, China. J. Environ. Monit. 14, 791-803.

Kong, S.F., Li, L., Li, X.X., Yin, Y., Chen, K., Liu, D.T., Yuan, L., Zhang, Y.J., Shan, Y.P., Ji, Y.Q., 2015. The impacts of firework burning at the Chinese Spring Festival on air quality: insights of tracers, source evolution and aging processes. Atmos. Chem. Phys. 15, 2167-2184.

Kumar, M., Singh, R.K., Murari, V., Singh, A.K., Singh, R.S. and Banerjee, T., 2016. Fireworks induced particle pollution: a spatio-temporal analysis. Atmospheric Res. 180, 78-91.

Li, Y.M., Pan, Y.P., Wang, Y.S., Wang, Y.F., Li, X.R., 2012. Chemical characteristics and sources of trace metals in precipitation collected from a typical industrial city in Northern China. Huan Jing Ke Xue 33(11), 3712-3717 (in Chinese).

López, J.M., Callén, M.S., Murillo, R., García, T., Navarro, M.V., de la Cruz, M.T., Mastral, A.M., 2005. Levels of selected metals in ambient air PM_{10} in an urban site of Zaragoza (Spain). Environ. Res. 99, 58–67.

Lough, G.C., Schauer, J.J., Park, J.S., Shafer, M.M., Deminter, J.T., Weinstein, J.P., 2005. Emissions of metals associated with motor vehicle roadways. Environ. Sci. Technol., 39, 826-836.

Lu, X., Zhang, X., Li, L. Y., Chen, H., 2014. Assessment of metals pollution and health risk in dust from nursery schools in Xi'an, China. Environ. Res. 128, 27-34.

Madrid, F., Barrientos, E.D., Madrid, L., 2008. Availability and bio-accessibility of metals in the clay fraction of urban soils of Sevilla. Environ. Pollut. 605-610.

Marcazzan, G.M., Vaccaro, S., Valli, G. and Vecchi, R., 2001. Characterisation of PM_{10} and $PM_{2.5}$ particulate matter in the ambient air of Milan (Italy). Atmos. Environ. 35(27), 4639-4650.

Meij, R., te Winkel, H., 2007. The emissions of heavy metals and persistent organic pollutants from modern coal-fired power stations. Atmos. Environ. 41(40), 9262-9272.

Ndiokwere, C.L., 1984. A study of heavy metal pollution from motor vehicle emissions and its effect on roadside soil, vegetation and crops in Nigeria. Environ. Pollut. B. 7(1), 35-42.

Pan, Y., Tian, S., Li, X., Ying, S., Yi, L., Wentworth, G.R., Wang, Y., 2015. Trace elements in particulate matter from metropolitan regions of northern China: sources, concentrations and size distributions. Sci. Total Environ. 537, 9-22.

Pongpiachan, S., 2013a. Diurnal variation, vertical distribution and source apportionment of carcinogenic polycyclic aromatic hydrocarbons (PAHs) in Chiang-Mai, Thailand. APJCP. 14(3), 1851-1863.

Pongpiachan, S., 2013b. Vertical distribution and potential risk of particulate polycyclic aromatic hydrocarbons in high buildings of Bangkok, Thailand. APJCP. 14(3), 1865-77.

Pongpiachan, S., 2016. Incremental lifetime cancer risk of $PM_{2.5}$ bound polycyclic aromatic hydrocarbons (PAHs) before and after the wildland fire episode. Aerosol Air Qual. Res, 16, 2907-2919.

Pongpiachan, S. and Iijima, A., 2016. Assessment of selected metals in the ambient air PM_{10} in urban sites of Bangkok (Thailand). ESPR. 23(3), 2948-2961.

Pongpiachan, S., Choochuay, C., Hattayanone, M., Kositanont, C., 2013. Temporal and spatial distribution of particulate carcinogens and mutagens in Bangkok, Thailand. APJCP. 14(3), 1879-1887.

Pongpiachan, S., Kositanont, C., Palakun, J., Liu, S., Ho, K.F., Cao, J. 2015a. Effects of day-of-week trends and vehicle types on $PM_{2.5}$-bounded carbonaceous compositions. Sci Total Environ. 532, 484-494.

Pongpiachan, S., Hattayanone, M., Choochuay, C., Mekmok, R., Wuttijak, N., Ketratanakul, A. 2015b. Enhanced PM_{10} bounded PAHs from shipping emissions. Atmos. Environ. 108, 13-19.

Pongpiachan, S., Hattayanone, M., Suttinun, O., Khumsup, C., Kittikoon, I., Hiruyatrakul, P., Cao, J., 2017a. Assessing human exposure to PM_{10}-bound polycyclic aromatic hydrocarbons during fireworks displays. APR. 8(5), 816-827.

Pongpiachan, S., Liu, S., Huang, R., Zhao, Z., Palakun, J., Kositanont, C., Cao, J., 2017b. Variation in day-of-week and seasonal concentrations of atmospheric $PM_{2.5}$-bound metals and associated health risks in Bangkok, Thailand. Arch. Environ. Contam. Toxicol. 1-16.

Pongpiachan, S., Mattanawadee, H., Junji, C., 2017c. Effect of agricultural waste burning season on PM 2.5-bound polycyclic aromatic hydrocarbon (PAH) levels in Northern Thailand. APR. 8(6), 1069-1080.

Pongpiachan, S., Hattayanone, M., Tipmanee, D., Suttinun, O., Khumsup, C., Kittikoon, I., Hirunyatrakul, P., 2017d. Chemical characterization of polycyclic aromatic hydrocarbons (PAHs) in 2013 Rayong oil spill-affected coastal areas of Thailand. Environ. Pollut. (In Press).

Ratcliffe, H.E., Swanson, G.M., Fischer, L.J., 1996. Human exposure to mercury: a critical assessment of the evidence of adverse health effects. J Toxicol Environ Health 49(3), 221-270.

Reddy, M.S., Basha, S., Joshi, H.V., Jha, B., 2005. Evaluation of the emission characteristics of trace metals from coal and fuel oil fired power plants and their fate during combustion. J. Hazard. Mater. 123(1), 242-249.

Rudnick, R.L., 2003. The Crust, Volume 3. Treatise on Geochemistry, Elsevier.

Samara, C., Voutsa, D., 2005. Size distribution of airborne particulate matter and associated heavy metals in the roadside environment. Chemosphere, 59(8), 1197-1206.

Seidel, D.J., Birnbaum, A.N., 2015. Effects of Independence Day fireworks on atmospheric concentrations of fine particulate matter in the United States. Atmos. Environ. 115, 192-198.

Sushil, S., Batra, V. S., 2006. Analysis of fly ash heavy metal content and disposal in three thermal power plants in India. Fuel, 85(17), 2676-2679.

Terzi, E., Argyropoulos, G., Bougatioti, A., Mihalopoulos, N., Nikolaou, K., Samara, C., 2010. Chemical composition and mass closure of ambient PM_{10} at urban sites. Atmos. Environ. 44, 2231-2239.

Tsai, H.H., Chien, L.H., Yuan, C.S., Lin, Y.C., Jen, Y.H., Ie, I.R., 2012. Influences of fireworks on chemical characteristics of atmospheric fine and coarse particles during Taiwan's Lantern Festival. Atmos. Environ. 62, 256-264.

Vecchi, R., Bernardoni, V., Cricchio, D., D'Alessandro, A., Fermo, P., Lucarelli, F., Nava, S., Piazzalunga, A., Valli, G., 2008. The impact of fireworks on airborne particles. Atmos. Environ. 42(6), 1121-1132.

Wang, Y., Zhuang, G., Xu, C., An, Z., 2007. The air pollution caused by the burning of fireworks during the lantern festival in Beijing. Atmos. Environ. 41(2), 417-431.

Wang, J., Hu, Z., Chen, Y., Chen, Z., Xu, S., 2013. Contamination characteristics and possible sources of PM_{10} and $PM_{2.5}$ in different functional areas of Shanghai, China. Atmos. Environ. 68, 221-229.

Wang, W., Cheng, S., Zhang, D., 2014. Association of inorganic arsenic exposure with liver cancer mortality: A meta-analysis. Environ. Res., 135, 120-125.

Wang, Y., Cheng, K., Wu, W., Tian, H., Yi, P., Zhi, G., Fan, J., Liu, S., 2017. Atmospheric emissions of typical toxic heavy metals from open burning of municipal solid waste in China. Atmos. Environ. 152, 6-15.

Warr, P., Menon, J., 2016. Cambodia's Special Economic Zones. JSEAE. 33(3), 273-290.

Weckwerth, G., 2001. Verification of traffic emitted aerosol components in the ambient air of Cologne (Germany). Atmos. Environ. 35(32), 5525-5536.

Winberry, W.T., Murphy, N.T., Riggin, R.M., 1988. Compendium of methods for the determination of toxic organic compounds in ambient air. Atmospheric Research and Exposure Assessment Laboratory, Office of Research and Development, US Environmental Protection Agency.

Wu, S., Peng, S., Zhang, X., Wu, D., Luo, W., Zhang, T., Zhou, S., Yang, G., Wan H., Wu, L., 2015. Levels and health risk assessments of heavy metals in urban soils in Dongguan, China. J Geochem Explor. 148, 71-78.

Yang, L.X., Gao, X.M., Wang, X.F., Nie, W., Wang, J., Gao, R., Xu, P.J., Shou, Y.P., Zhang, Q.Z., Wang, W.X., 2014. Impacts of firecracker burning on aerosol chemical characteristics and human health risk levels during the Chinese New Year celebration in Jinan, China. Sci. Total Environ. (476-477), 57-64.

Yatkin, S., Bayram, A., 2008a. Determination of major natural and anthropogenic source profiles for particulate matter and trace elements in Izmir, Turkey. Chemosphere, 71, 685-696.

Yatkin, S., Bayram, A., 2008b. Source apportionment of PM_{10} and $PM_{2.5}$ using positive matrix factorization and chemical mass balance in Izmir, Turkey. Sci. Total Environ. 390, 109-123.

Yoo, J.I., Kim, K.H., Jang, H.N., Seo, Y.C., Seok, K.S., Hong, J.H., Jang, M., 2002. Emission characteristics of particulate matter and heavy metals from small incinerators and boilers. Atmos. Environ. 36(32), 5057-5066.

Zhang, H., He, P.J., Shao, L.M., 2008. Fate of heavy metals during municipal solid waste incineration in Shanghai. J. Hazard. Mater. 156(1), 365-373.

Zhang, H., Wang, Z., Zhang, Y., Ding, M., Li, L., 2015. Identification of traffic-related metals and the effects of different environments on their enrichment in roadside soils along the Qinghai-Tibet highway. Sci. Total. Environ. (521-522C), 160-172.

666

667 Table 1. Statistical description of concentrations of 31 selected metals (ng m^{-3}) in PM_{10} during FDP
668 and NDP
669

	FDP	NDP	T-Test
	Conc. [ng m^{-3}]	Conc. [ng m^{-3}]	(p<0.05)
Li	0.852 (0.425~1.26)	0.844 (0.280~1.63)	NS*
Be	0.0614 (0.0444~0.0766)	0.0624 (0.0300~0.100)	NS
Na	1,374 (198~2,855)	1,339 (77.6~3,006)	NS
Mg	263 (26.5~492)	330 (109~641)	NS
Al	722 (N.D. ~1,028)	883 (237~1,768)	S**
K	1,206 (741~1,969)	1,094 (199~2,542)	NS
Ca	2,096 (1,219~2,977)	2,794 (973~5,274)	S
Sc	0.160 (0.0751~0.210)	0.196 (0.0800~0.360)	S
V	5.97 (3.20~12.1)	4.67 (1.38~11.15)	NS
Cr	2.03 (0.600~7.05)	3.58 (0.220~27.10)	S
Mn	39.6 (20.2~64.0)	41.1 (12.2~93.6)	NS
Fe	922 (569~1,167)	997 (380~1,446)	NS
Co	0.391 (0.212~0.546)	0.393 (0.140~0.690)	NS
Ni	4.16 (2.18~7.30)	3.16 (0.670~6.59)	NS
Cu	133 (85.8~264)	163 (45.9~410)	NS
Zn	233 (123~411)	189 (35.4~496)	NS
As	7.00 (2.35~13.3)	6.32 (0.950~22.4)	NS
Se	3.52 (0.916~6.12)	3.24 (0.590~10.4)	NS
Rb	5.09 (2.57~8.22)	4.99 (1.27~11.0)	NS
Sr	8.05 (3.44~20.7)	7.04 (2.63~13.7)	NS
Y	0.347 (N.D. ~0.506)	0.465 (0.220~0.870)	S
Zr	7.95 (5.55~11.8)	8.54 (3.64~12.5)	NS
Mo	4.11 (0.757~15.1)	5.15 (0.0300~17.6)	NS
Cd	1.80 (0.289~3.26)	1.40 (0.260~3.89)	NS
Sn	9.55 (4.62~20.6)	8.85 (2.26~17.5)	NS
Sb	10.1 (5.33~15.2)	9.43 (3.01~28.8)	NS
Cs	0.239 (0.0347~0.458)	0.237 (N.D. ~0.710)	NS
Ba	68.1 (38.3~106)	57.0 (19.5~95.6)	S
Tl	0.334 (0.0357~0.798)	0.295 (0.0400~1.19)	NS
Pb	74.7 (29.2~145)	47.2 (7.96~119)	S
Bi	1.82 (0.449~4.63)	1.83 (0.310~6.89)	NS

670 *NS: Non-significant
671 **S: Significant
672
673

Preprints (www.preprints.org) | NOT PEER-REVIEWED | Posted: 20 March 2018 doi:10.20944/preprints201803.0171.v1

Peer-reviewed version available at Atmosphere 2018, 9, 144; doi:10.3390/atmos9040144

674
675 Table 2. Mean ratios of selected metals representative of FDP and NDP
676

Diagnostic Binary Ratios	FDP	NDP	FDP/NDP
Pb/Ca	0.036	0.017	2.1
Pb/Na	0.054	0.035	1.5
Pb/K	0.062	0.043	1.4
Pb/Fe	0.081	0.047	1.7
Pb/Al	0.10	0.053	1.9
Pb/Mg	0.28	0.14	2.0
Pb/Zn	0.32	0.25	1.3
Pb/Cu	0.56	0.29	1.9
Ba/Ca	0.033	0.020	1.6
Ba/Na	0.050	0.043	1.2
Ba/K	0.057	0.052	1.1
Ba/Fe	0.074	0.057	1.3
Ba/Al	0.094	0.065	1.5
Ba/Mg	0.26	0.17	1.5
Ba/Zn	0.29	0.30	1.0
Ba/Cu	0.51	0.35	1.5
Li/Cs	3.6	3.56	1.00
Li/Tl	2.6	2.86	0.89
Al/Y	2077	1897	1.09
V/Ni	1.4	1.5	0.97
Mn/Cs	165	173	0.96
Mn/Tl	119	139	0.85
Cu/Mo	32	32	1.03
Cu/Sb	13	17	0.8
Cd/Cu	0.014	0.0086	1.6
Cd/Pb	0.024	0.030	0.8
Se/Cd	2.0	2.3	0.8

677
678
679
680
681
682
683

Table 3. Hazard quotients, hazard indexes, and cancer risks for selected metals present in PM_{10} in Bangkok

	FDP				NDP					FDP	NDP		FDP	NDP
Elements	$D_{inh\text{-}children}$	$D_{inh\text{-}adults}$	$HQ_{children}$	HQ_{adult}	$D_{inh\text{-}children}$	$D_{inh\text{-}adults}$	$HQ_{children}$	HQ_{adult}	R_f	*LADD*	*LADD*	SF_a	*R*	*R*
Pb	1.72E-07	9.67E-08	4.87E-05	2.75E-05	1.08E-07	6.12E-08	3.08E-05	1.74E-05	3.52E-03	1.27E-04	8.03E-05			
Cr	4.65E-09	2.62E-09	1.63E-04	9.17E-05	8.22E-09	4.63E-09	2.87E-04	1.62E-04	2.86E-05	3.44E-06	6.08E-06	42	1.45E-04	2.56E-04
Co	8.97E-10	5.06E-10	1.57E-04	8.86E-05	9.03E-10	5.09E-10	1.58E-04	8.92E-05	5.71E-06	6.65E-07	6.69E-07	9.8	6.51E-06	6.55E-06
Ni	9.56E-09	5.39E-09	4.64E-07	2.62E-07	7.26E-09	4.09E-09	3.52E-07	1.99E-07	2.06E-02	7.08E-06	5.37E-06	0.84	5.94E-06	4.51E-06
Zn	5.34E-07	3.01E-07	1.77E-06	1.00E-06	4.34E-07	2.45E-07	1.44E-06	8.14E-07	3.01E-01	3.95E-04	3.22E-04			
As	1.61E-08	9.07E-09	5.34E-05	3.01E-05	1.45E-08	8.19E-09	4.82E-05	2.72E-05	3.01E-04	1.19E-05	1.07E-05	15.1	1.80E-04	1.62E-04
Cd	4.13E-09	2.33E-09	4.13E-06	2.33E-06	3.21E-09	1.81E-09	3.21E-06	1.81E-06	1.00E-03	3.06E-06	2.38E-06	6.4	1.96E-05	1.52E-05
V	1.37E-08	7.73E-09	1.96E-06	1.10E-06	1.07E-08	6.04E-09	1.53E-06	8.63E-07	7.00E-03	1.02E-05	7.94E-06			
Mn	9.09E-08	5.12E-08	6.49E-03	3.66E-03	9.44E-08	5.33E-08	6.75E-03	3.80E-03	1.40E-05	6.73E-05	6.99E-05			
Σ	8.46E-07	4.77E-07	6.92E-03	3.90E-03	6.82E-07	3.85E-07	7.28E-03	4.10E-03		6.26E-04	5.05E-04		3.57E-04	4.44E-04

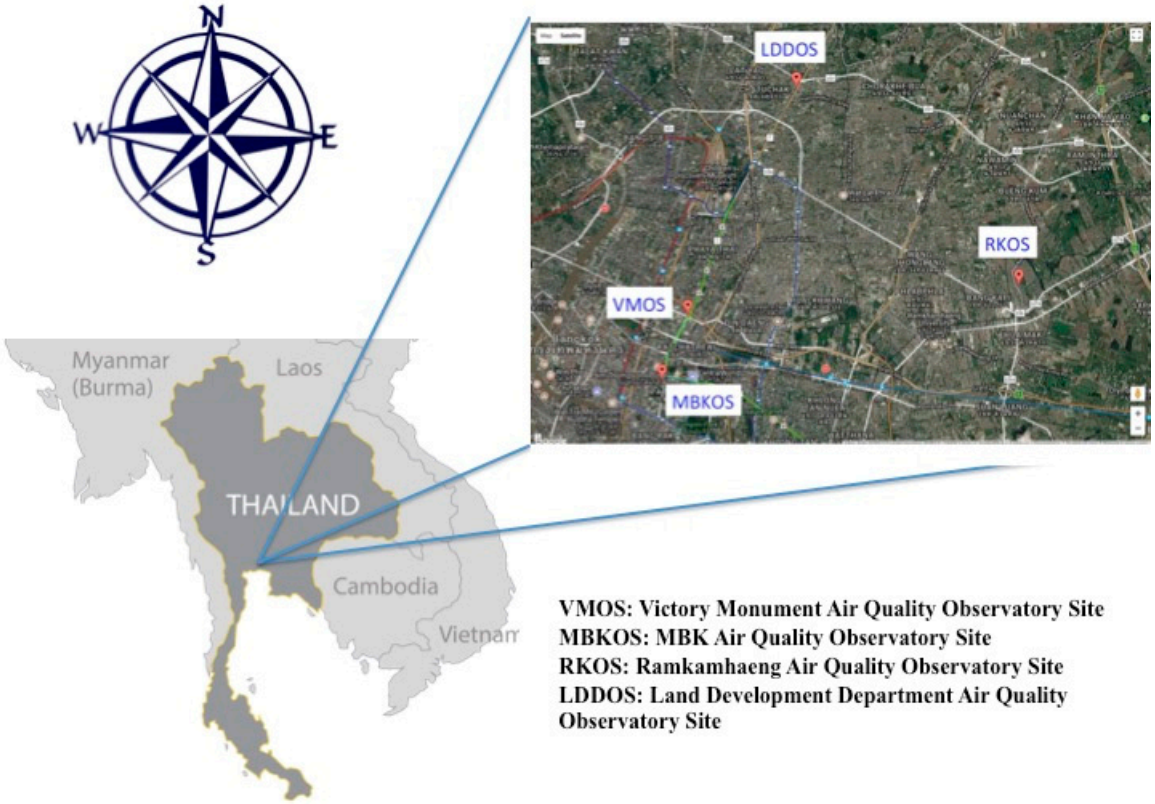

Fig. 1. Locations of four PCD air quality observation sites, Bangkok

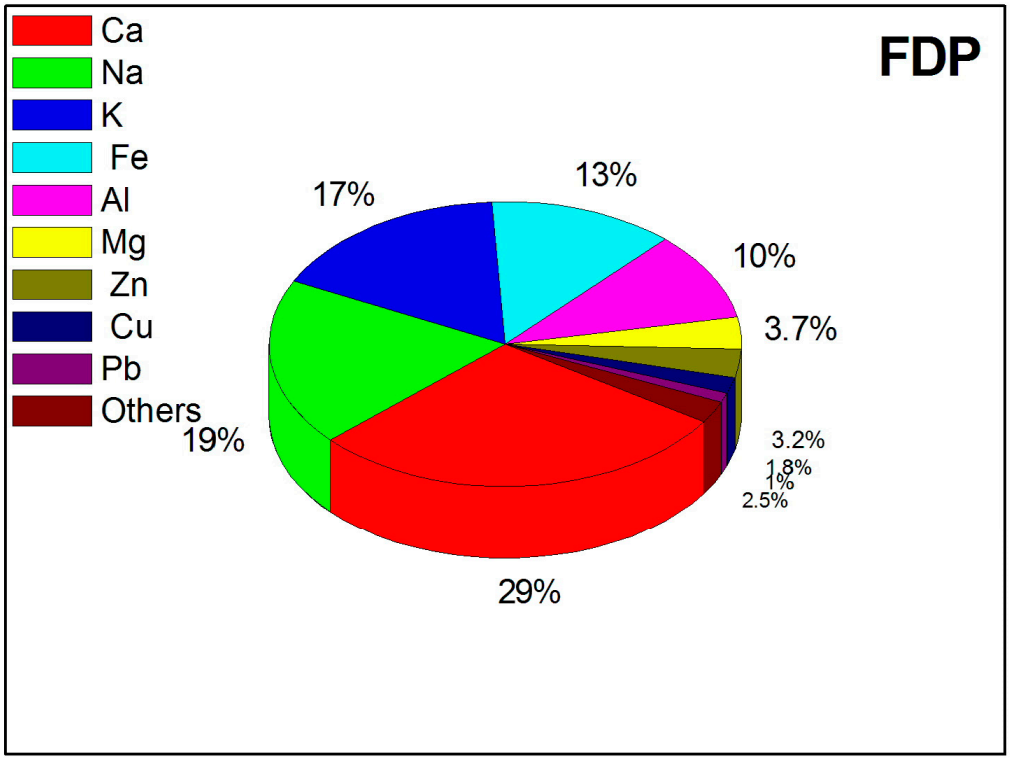

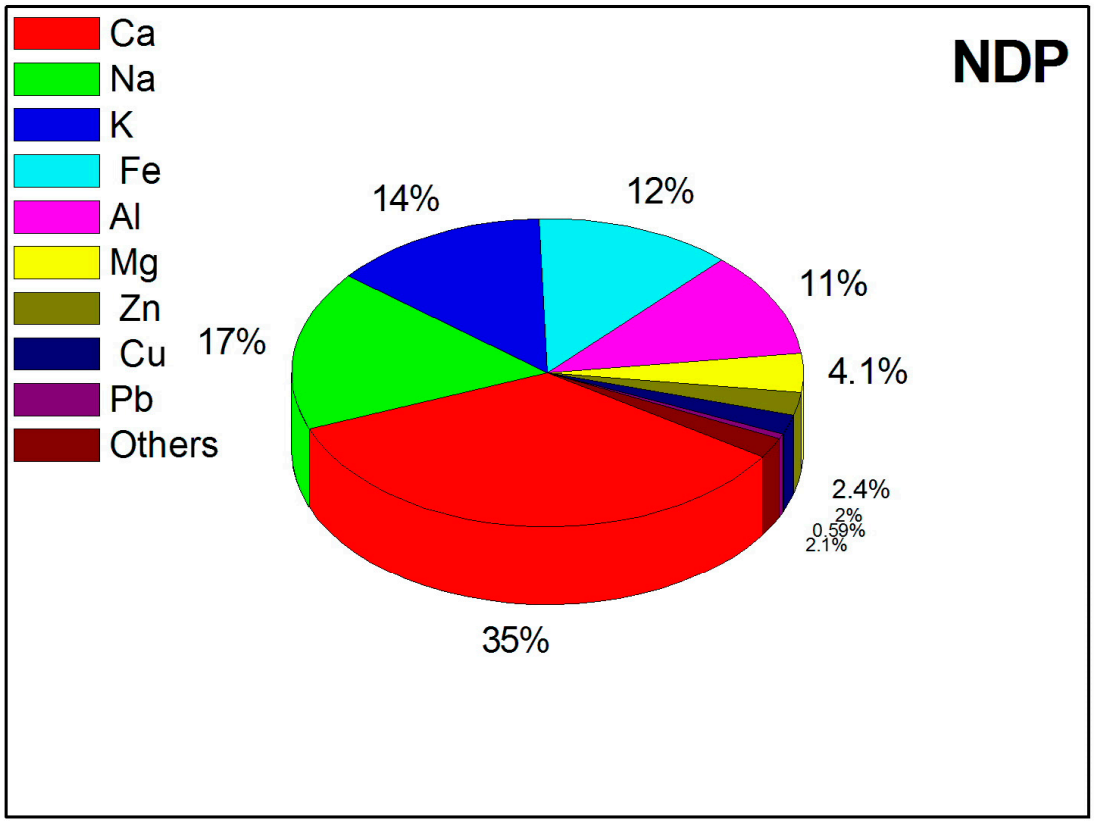

Fig. 2. Percentage contributions of selected metals collected during FDP and NDP

Preprints (www.preprints.org) | NOT PEER-REVIEWED | Posted: 20 March 2018 doi:10.20944/preprints201803.0171.v1

Peer-reviewed version available at Atmosphere 2018, 9, 144; doi:10.3390/atmos9040144

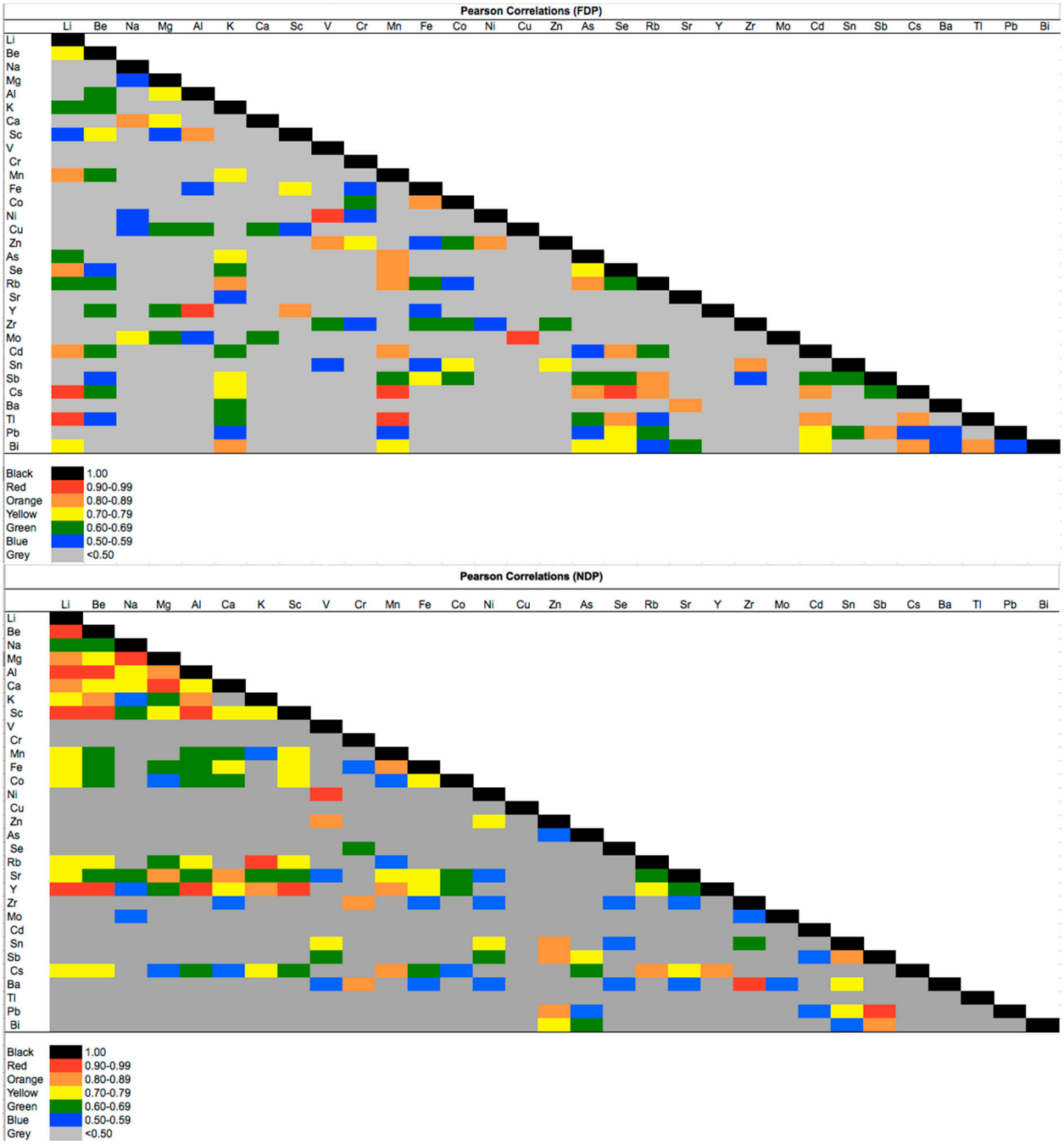

Fig. 3. Pearson correlation analysis of 31 selected metals collected during FDP and NDP

Peer-reviewed version available at Atmosphere 2018, 9, 144; doi:10.3390/atmos9040144

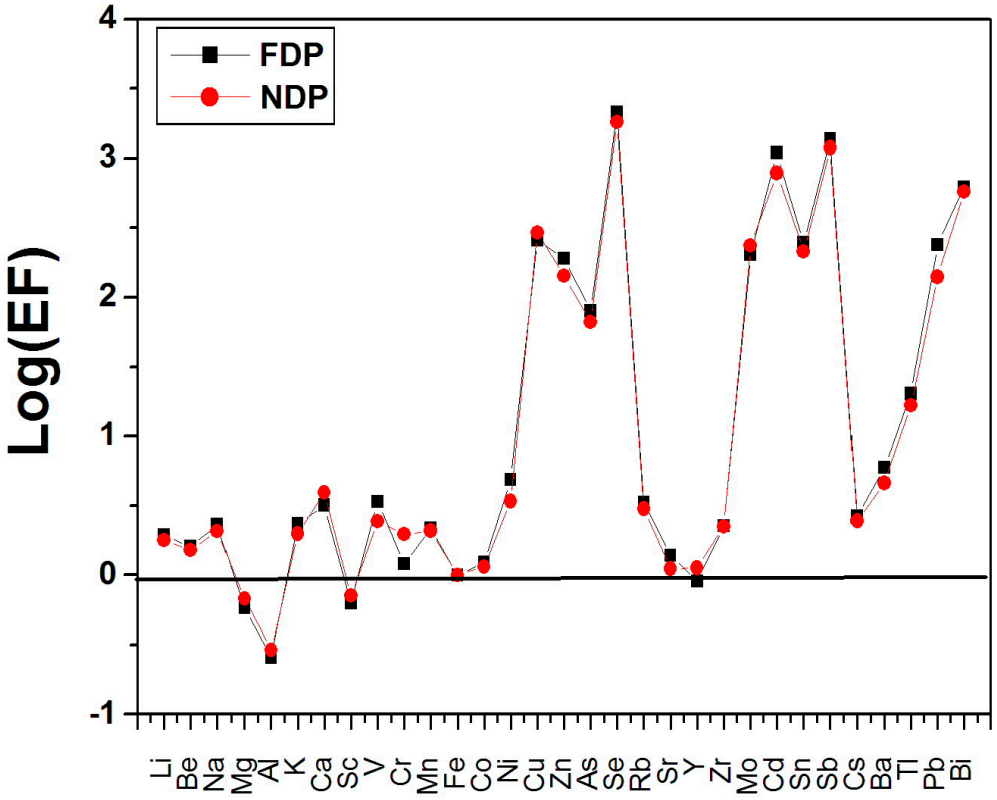

Fig. 4. Logarithms of enrichment factors for 31 selected metals collected during FDP and NDP

Preprints (www.preprints.org) | NOT PEER-REVIEWED | Posted: 20 March 2018 doi:10.20944/preprints201803.0171.v1

Peer-reviewed version available at Atmosphere 2018, 9, 144; doi:10.3390/atmos9040144

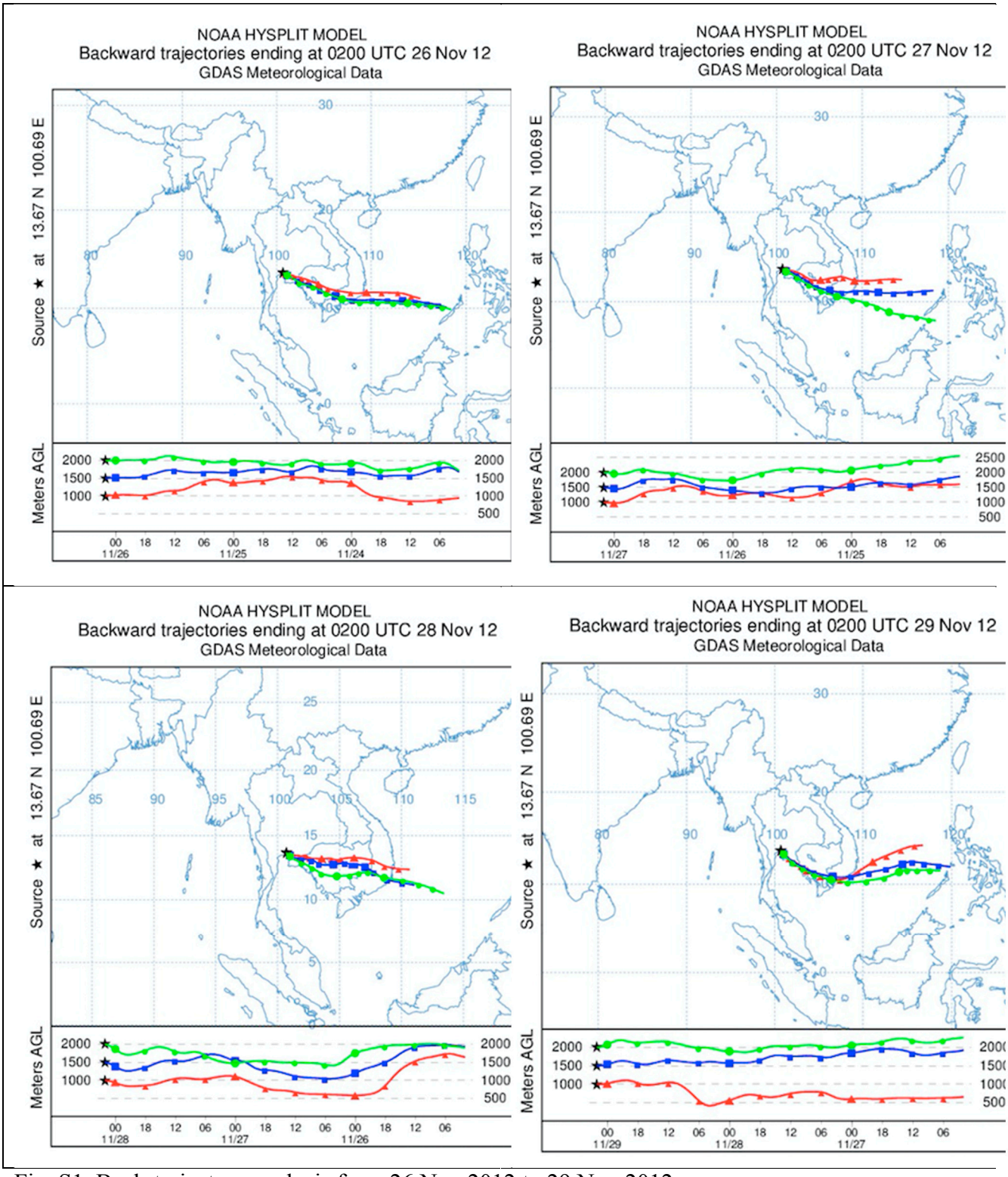

Fig. S1. Back-trajectory analysis from 26 Nov 2012 to 29 Nov 2012

Preprints (www.preprints.org) | NOT PEER-REVIEWED | Posted: 20 March 2018 doi:10.20944/preprints201803.0171.v1

Peer-reviewed version available at Atmosphere 2018, 9, 144; doi:10.3390/atmos9040144

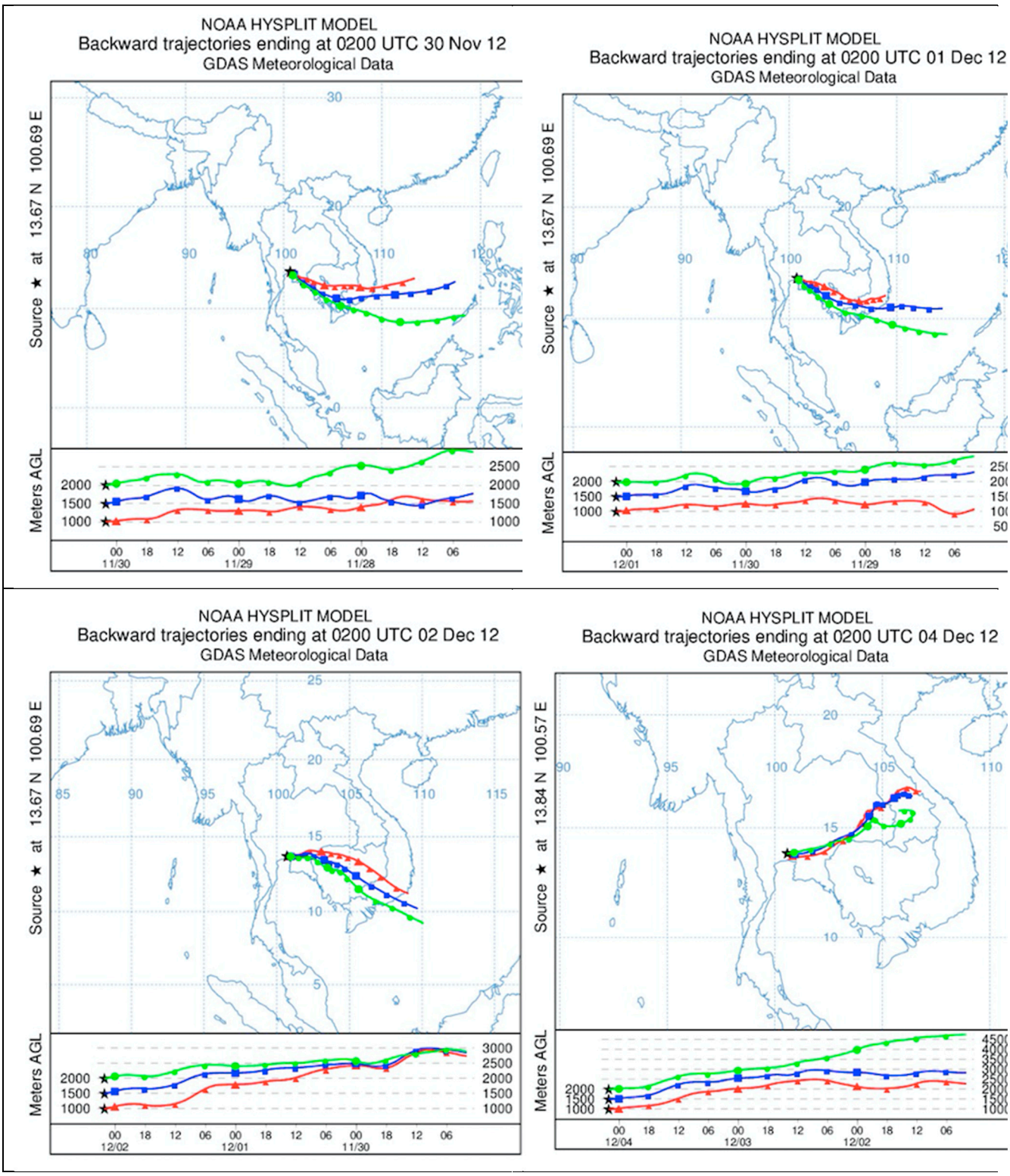

Fig. S2. Back-trajectory analysis from 30 Nov 2012 to 4 Dec 2012

Preprints (www.preprints.org) | NOT PEER-REVIEWED | Posted: 20 March 2018 doi:10.20944/preprints201803.0171.v1

Peer-reviewed version available at Atmosphere 2018, 9, 144; doi:10.3390/atmos9040144

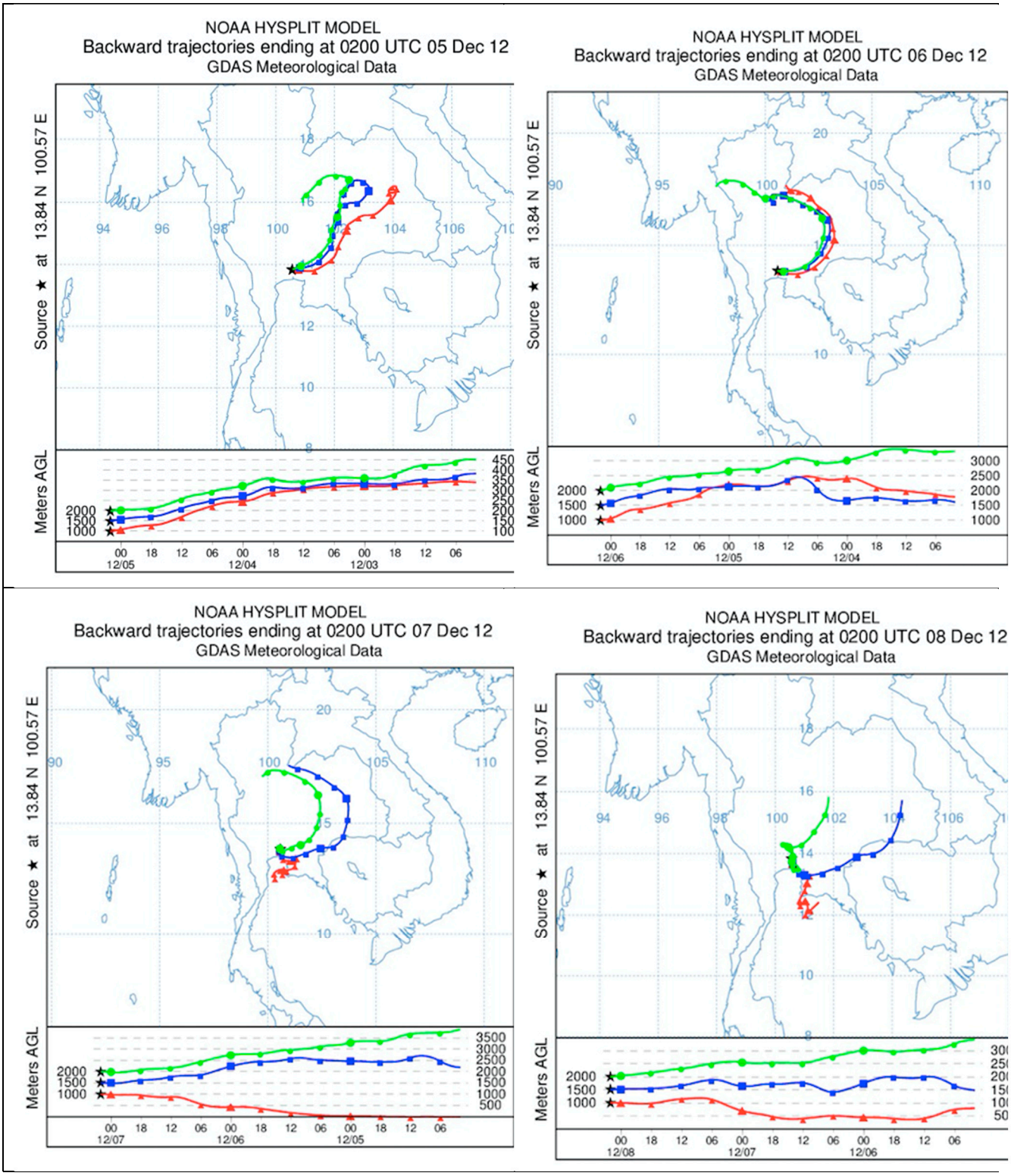

Fig. S3. Back-trajectory analysis from 5 Dec 2012 to 8 Dec 2012

Preprints (www.preprints.org) | NOT PEER-REVIEWED | Posted: 20 March 2018 doi:10.20944/preprints201803.0171.v1

Peer-reviewed version available at Atmosphere 2018, 9, 144; doi:10.3390/atmos9040144

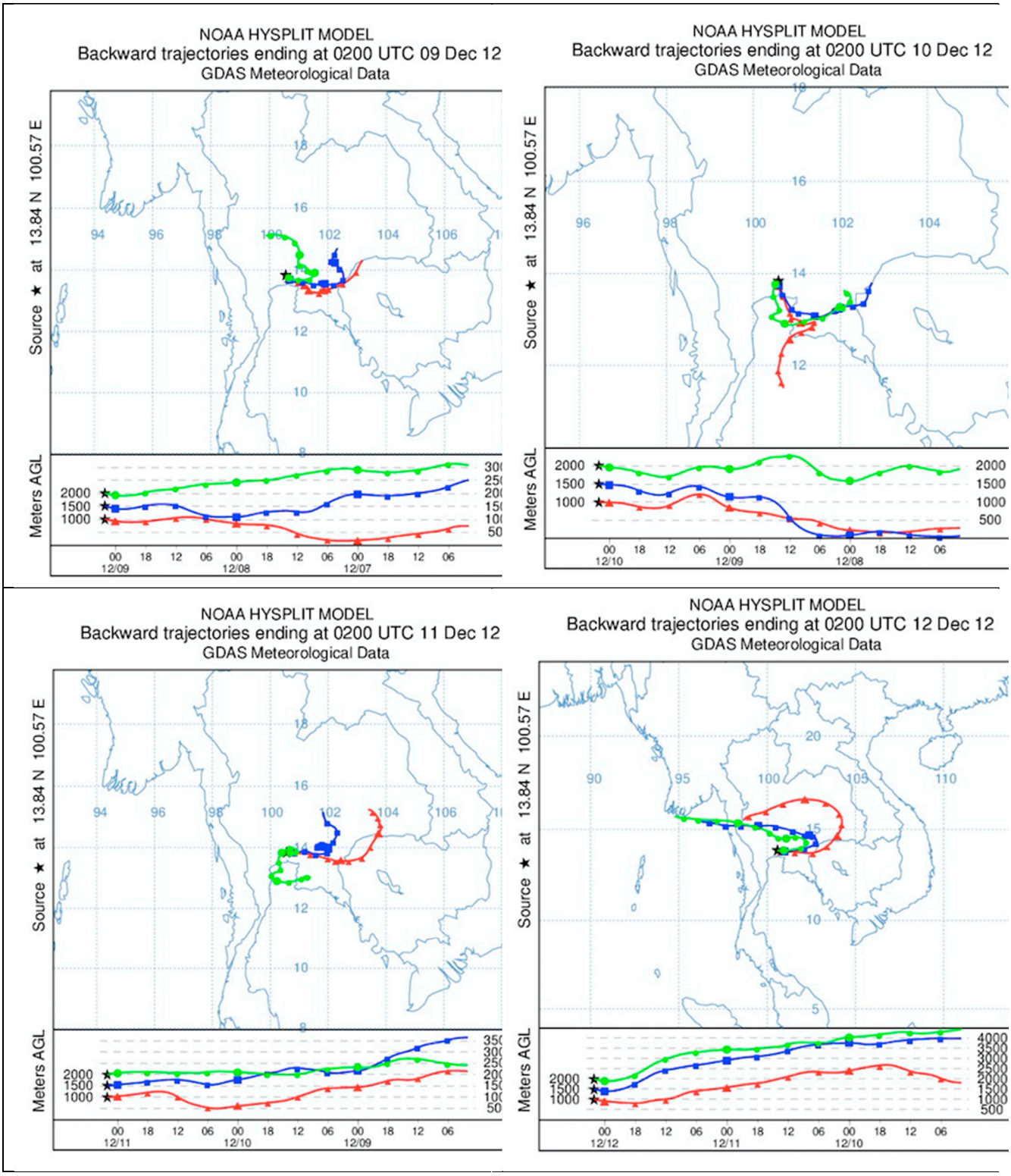

Fig. S4. Back-trajectory analysis from 9 Dec 2012 to 12 Dec 2012

Preprints (www.preprints.org) | NOT PEER-REVIEWED | Posted: 20 March 2018 doi:10.20944/preprints201803.0171.v1

Peer-reviewed version available at Atmosphere 2018, 9, 144; doi:10.3390/atmos9040144

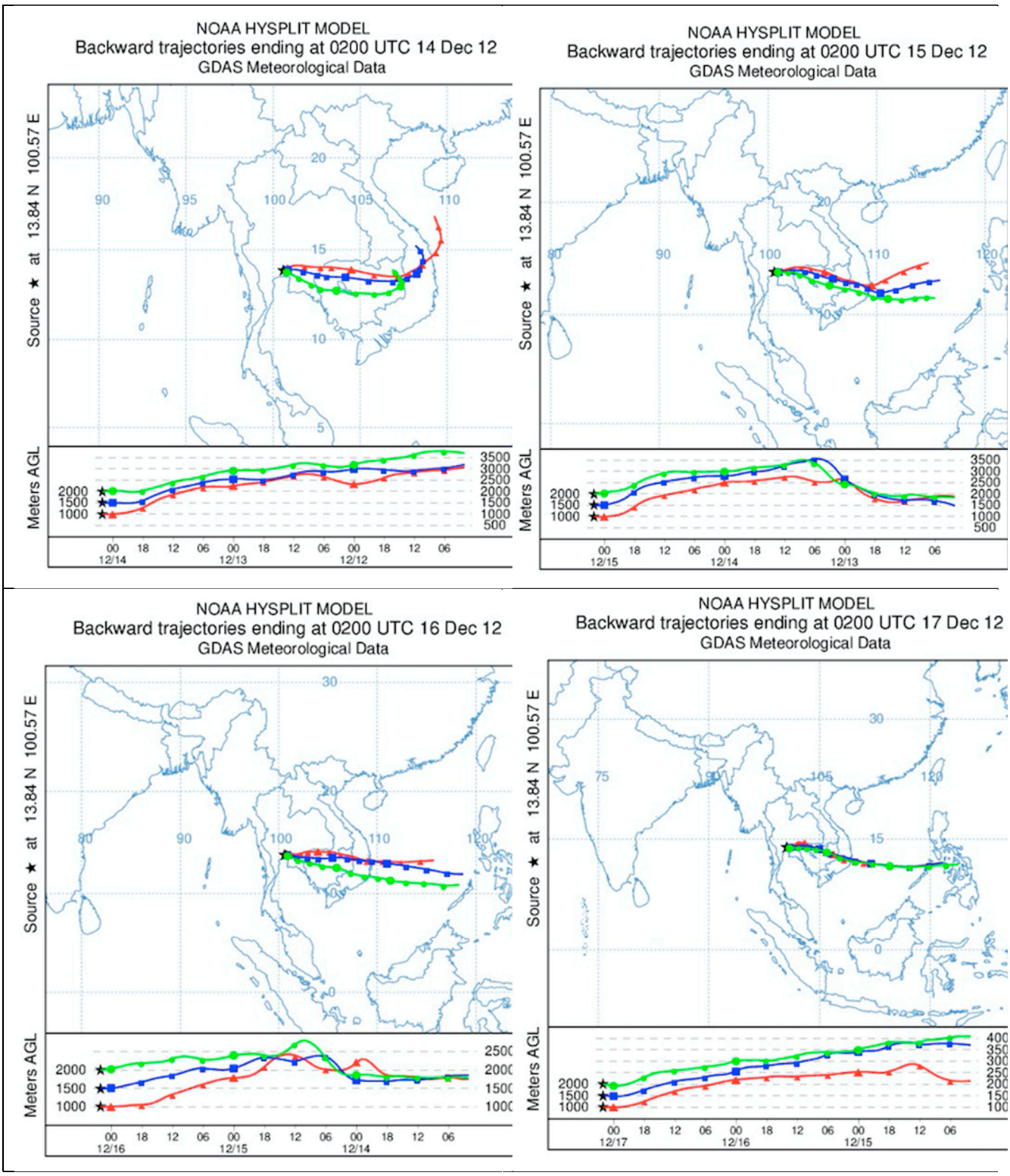

Fig. S5. Back-trajectory analysis from 14 Dec 2012 to 17 Dec 2012

Preprints (www.preprints.org) | NOT PEER-REVIEWED | Posted: 20 March 2018 doi:10.20944/preprints201803.0171.v1

Peer-reviewed version available at Atmosphere 2018, 9, 144; doi:10.3390/atmos9040144

Table S1. Analytical performance obtained by ICP-MS.

Element	Analytical Mode[a]	Mass/Charge	Detection Limit[b]	Unit	Standard Solution
Li	NG	7	4.72	ng L^{-1}	XSTC-331
Be	NG	9	2.70	ng L^{-1}	XSTC-331
Na	H2	23	1.30	µg L^{-1}	XSTC-331
Mg	He	24	0.427	µg L^{-1}	XSTC-331
Al	He	27	0.117	µg L^{-1}	XSTC-331
K	H2	39	1.02	µg L^{-1}	XSTC-331
Ca	H2	40	0.601	µg L^{-1}	XSTC-331
Sc	He	45	1.35	ng L^{-1}	XSTC-1
V	He	51	0.927	ng L^{-1}	XSTC-331
Cr	He	53	5.28	ng L^{-1}	XSTC-331
Mn	He	55	9.11	ng L^{-1}	XSTC-331
Fe	He	56	73.9	ng L^{-1}	XSTC-331
Co	He	59	0.937	ng L^{-1}	XSTC-331
Ni	He	60	10.6	ng L^{-1}	XSTC-331
Cu	He	63	15.0	ng L^{-1}	XSTC-331
Zn	He	66	40.0	ng L^{-1}	XSTC-331
As	He	75	2.66	ng L^{-1}	XSTC-331
Se	H2	78	11.5	ng L^{-1}	XSTC-331
Rb	He	85	4.13	ng L^{-1}	XSTC-331
Sr	He	88	1.96	ng L^{-1}	XSTC-331
Y	He	89	2.50	ng L^{-1}	XSTC-1
Zr	He	90	0.171	ng L^{-1}	XSTC-8
Mo	He	95	1.75	ng L^{-1}	XSTC-8
Cd	He	111	2.25	ng L^{-1}	XSTC-331
Sn	He	118	1.53	ng L^{-1}	XSTC-7
Sb	He	121	0.494	ng L^{-1}	XSTC-7
Cs	He	133	0.922	ng L^{-1}	XSTC-331
Ba	He	137	2.13	ng L^{-1}	XSTC-331
Tl	He	205	0.657	ng L^{-1}	XSTC-331
Pb	He	208	1.44	ng L^{-1}	XSTC-331
Bi	He	209	10.5	ng L^{-1}	XSTC-331

[a] Determination was performed under three different analytical modes. NG = non-gas mode, which was performed without collision/reaction cell system.

[b] Values were defined as three times the standard deviation of ten calibration blank analyses. H_2 = reaction mode using hydrogen gas. He = collision mode using helium gas.